

# Clusterization in D-optimal designs: the case against linearization

Yair Daon\* 

**Abstract.** Estimation of parameters in physical processes often demands costly measurements, prompting the pursuit of an optimal measurement strategy. Finding such strategy is termed the problem of optimal experimental design, abbreviated as optimal design. Remarkably, optimal designs can yield tightly clustered measurement locations, leading researchers to fundamentally revise the design problem just to circumvent this issue. Some authors introduce error correlation among error terms that are initially independent, while others restrict measurement locations to a finite set of locations. While both approaches may prevent clusterization, they also fundamentally alter the optimal design problem.

In this study, we consider Bayesian D-optimal designs, i.e. designs that maximize the expected Kullback-Leibler divergence between posterior and prior. We propose an analytically tractable model for D-optimal designs over Hilbert spaces. In this framework, we make several key contributions: (a) We establish that measurement clusterization is a generic trait of D-optimal designs for linear inverse problems with independent Gaussian measurement errors and a Gaussian prior. (b) We prove that introducing correlations among measurement error terms mitigates clusterization. (c) We characterize D-optimal designs as reducing uncertainty across a subset of prior covariance eigenvectors. (d) We leverage this characterization to argue that measurement clusterization arises as a consequence of the pigeonhole principle: when more measurements are taken than there are locations where the select eigenvectors are large and others are small — clusterization occurs. Finally, we use our analysis to argue against the use of Gaussian priors with linearized physical models when seeking a D-optimal design.

**MSC2020 subject classifications:** Primary 62F15, 35R30; secondary 28C20.

**Keywords:** D-optimal design, inverse problem, clusterization.

## 1 Introduction

Experimental design is a systematic approach to specifying every possible aspect of an experiment [10]. In this study, we focus on experiments that involve measuring quantities arising from naturally occurring processes. For us, therefore, experimental design entails determining which specific measurements to record from a given process. In a typical experiment the number of measurements that can be recorded is limited by time, cost and other constraints. Therefore selecting the right set of measurements to record is crucial as it directly impacts the utility of the data collected, and consequently, the validity of the conclusions drawn.

---

\*Azrieli Faculty of Medicine, Bar-Ilan University, Safed, Israel , [firstname.lastname@gmail.com](mailto:firstname.lastname@gmail.com)

For example, consider the process of searching for oil: measurements require digging deep holes in the ground, known as "boreholes". A *design* simply indicates which boreholes should be dug [17]. Since digging boreholes is expensive, only a limited number of them can be dug, and thus carefully choosing their locations is crucial.

Specifying the right set of measurements holds particular significance when solving an *inverse problem* — i.e. making inference of the physical world utilizing a physical model of a phenomenon of interest [41, 21]. In an inverse problem, we seek to infer physical quantities, based on observations and a model of the physical world. Models are typically phrased in the language of ordinary or partial differential equations.

Inverse problems are ubiquitous in science and engineering. For example, in electrical impedance tomography (EIT) we seek to infer the structure of the inside of a human body. Inference is conducted based on observations of electrical current impedance measured at specific electrode locations on the skin, leveraging known equations of electric current flow [18]. Magnetic Resonance Imaging (MRI) also entails solving an inverse problem. There, radio-frequency pulses are sent through the human body in the presence of a strong magnetic field. The response of one's body contents to these radio-frequency pulses is measured, allowing a radiologist to view the internals of a body in a noninvasive manner [27]. An inverse problem also arises in oil and gas exploration, where acoustic waves are sent through "boreholes" — deep cylindrical wells drilled into the ground. Data of travel and return times of the acoustic waves are recorded. Wave travel and return time is influenced by the properties of the subsurface materials, such as density, elasticity, and the presence of fluids or voids. Combining travel time data with a geophysical model of the contents of the earth's crust facilitates reconstructing the structure of the subsurface in a process called *borehole tomography* [17]. Inverse problems also arise in many other areas of seismology and geology [34, 39] and medical imaging [41]. In many inverse problems the goal is to infer some numerical parameter. However, in the formulation we consider in this study, as well as in the examples above, the goal is to conduct inference over some *function* over  $\Omega$ , where  $\Omega \subseteq \mathbb{R}^d$ ,  $d = 1, 2, 3$  is a spatial domain of interest.

## 1.1 D-optimal Designs

In all of the examples of inverse problems we have seen, as well as in many other applications, only a limited number of measurements are allowed. For example, in borehole tomography, a measurement involves drilling a deep well in the ground — a very costly endeavor. In medical imaging applications like MRI, the time allotted for each patient in the MRI machine limits the number of measurements that can be taken during a single session. Therefore, measurements should be chosen to extract as much information from the experiment. Typically, a user will consider some utility, called a *design criterion* and take measurements that maximize this utility. Two of the most widely recognized and extensively studied design criteria are the A- and *D-optimality* criteria.

In this study, we focus on the Bayesian D-optimality criterion. Bayesian D-optimality carries a simple and intuitive meaning: measurements chosen according to the D-optimality criterion maximize the expected Kullback-Leibler (KL) divergence from posterior to

prior [10, 1, 12]. Recall that for a discrete parameter  $\mathbf{m}$  and data  $\mathbf{d}$ , the KL divergence is defined as

$$D_{KL}(\Pr(\mathbf{m}|\mathbf{d})||\Pr(\mathbf{m})) = \sum_{\mathbf{m}} \log \frac{\Pr(\mathbf{m}|\mathbf{d})}{\Pr(\mathbf{m})} \Pr(\mathbf{m}|\mathbf{d}). \quad (1)$$

Of course, data  $\mathbf{d}$  is not known before the experiment is conducted. Hence, we average over  $\mathbf{d}$  to define the D-optimality criterion as:

$$\mathbb{E}_{\mathbf{d}} [D_{KL}(\Pr(\mathbf{m}|\mathbf{d})||\Pr(\mathbf{m}))].$$

We refer to a set of measurements that maximizes the D-optimality criterion as a *D-optimal design*.

For a linear model with Gaussian prior in finite dimensions, a D-optimal design minimizes the determinant of the posterior covariance [10]. In Section 2.3 we give a more general definition of the D-optimality criterion that applies to arbitrary measures. We also show how the D-optimality criterion generalizes to linear models over infinite-dimensional Hilbert spaces (e.g. function spaces).

## 1.2 A toy model: the 1D heat equation

For concreteness, let us now consider a toy inverse problem: inferring the initial condition for a partial differential equation known as the *heat equation* in one dimension (1D heat equation henceforth). Readers less familiar with partial differential equations can think of the following setup: before us there is a metal rod, perfectly insulated except for its tips. At each point on the rod the temperature is different and unknown, and we call this temperature distribution the *initial condition*. We wait for a short time  $T$  and let the heat dissipate a bit inside the rod. The heat equation determines the heat distribution inside the rod at time  $t = T$ .

The full time evolution of heat in the rod  $\Omega = [0, 1]$  is formally described by the following three equations:

$$u_t = \Delta u \quad \text{in } [0, 1] \times [0, \infty), \quad (2a)$$

$$u = 0 \quad \text{on } \{0, 1\} \times [0, \infty), \quad (2b)$$

$$u = u_0 \quad \text{on } [0, 1] \times \{0\}. \quad (2c)$$

As time passes, heat dissipates across the rod as hotter regions, e.g. local maxima of the heat distribution, become cooler. This behavior is captured by eq. (2a): the Laplacian at local maxima is negative, so  $u_t = \Delta u$  implies  $u$  decreases at its maxima, and the reverse happens at local minima. Eq. (2b) describes the *boundary condition*, which dictates how heat interacts with the outside world at the two edges of the rod  $\{0, 1\}$ . Specifically, eq. (2b) implements an absorbing boundary, i.e. heat that interacts with the boundary immediately disappears. This type of boundary condition is known as a *homogeneous Dirichlet boundary condition*. Eq. (2c) describes the *initial condition*, i.e. the heat distribution inside the rod at time  $t = 0$ .

Solving the 1D heat equation is straightforward. Consider an initial heat distribution  $u_0 \in L^2([0, 1])$  that satisfies the homogeneous Dirichlet boundary condition

eq. (2b). This initial condition  $u_0$  is a linear combination of sines  $\mathbf{e}_n(x) = \sin(\pi nx)$ , so  $u_0 = \sum_{n \geq 1} a_n \mathbf{e}_n$  for some  $\{a_n\}_{n \geq 1}$ . Now, note that  $\mathbf{e}_n$  are in fact eigenvectors of the Laplacian:  $\Delta \mathbf{e}_n = -\pi^2 n^2 \mathbf{e}_n$ . It should not be hard to believe that  $u(\cdot, T) = \sum_{n \geq 1} a_n \exp(-\pi^2 n^2 T) \mathbf{e}_n$  [35]. Thus, eigenvectors of the linear operator that describes the time evolution of heat are  $\mathbf{e}_n(x) = \sin(\pi nx)$  with corresponding eigenvalues

$$\exp(-\pi^2 n^2 T). \quad (3)$$

In the *inverse problem of the 1D heat equation*, our goal is to infer the initial condition  $u_0 = u(\cdot, 0)$  from noisy observations of the final state  $u(\cdot, T)$ . However, we are not able to measure  $u(\cdot, T)$  at every point in the domain  $\Omega$ . Rather, we take some number of temperature measurements on the rod once our waiting time  $T$  has passed and try to infer  $u(\cdot, 0)$  from these measurements.

The inverse problem of the 1D heat equation is difficult ("ill-posed") since heat spreads in a diffusive manner and any roughness in the initial condition is quickly smoothed, as implied by the squared exponential decay of eigenvalues in eq. (3) with  $n \rightarrow \infty$ . See Supplementary movies S1 and S2 for an illustration of this phenomenon<sup>1</sup>. For ill-posed problems regularization is required, and we implement such regularization via a fully Bayesian formulation of the inverse problem.

In order to find a fully Bayesian formulation for our inverse problem we first need to specify a prior on *functions* defined over  $\Omega = [0, 1]$ . For the sake of simplicity we would like to utilize a Gaussian prior. While specifying the prior mean is easy — we take the zero function on  $\Omega$  — specifying a prior covariance is more involved. In analogy with the finite dimensional case, we seek a covariance *operator* that is positive definite and imposes sufficient regularity on functions over  $\Omega$ . Thus, we set our prior for the initial condition  $u_0 \sim \mathcal{N}(0, (-\Delta)^{-1})$ , where  $\Delta$  is again defined with a homogeneous Dirichlet boundary condition. The intuition here is that since  $\Delta$  is a differential operator, it is "roughing" (the opposite of smoothing) and so  $(-\Delta)^{-1}$  is smoothing. Prior realizations are generated, in analogy to the finite dimensional case, by smoothing white noise:  $(-\Delta)^{-1/2} \mathcal{W}$ , where  $\mathcal{W}$  is white noise [25]. Our choice of prior covariance operator ensures the posterior is well-defined and prior realizations are well-behaved, see Theorem 3.1 and Lemma 6.25 in [40] for details. The second ingredient of a fully Bayesian formulation of the inverse problem is likelihood. We simply assume centered iid Gaussian measurement error model, giving rise to a the widely applicable Gaussian likelihood function.

Now that we have a fully Bayesian formulation of our toy inverse problem, we would like to find a D-optimal design. Defining D-optimal designs over function spaces is somewhat mathematically involved. Thus, to keep our discussion here focused, we will explore these technical details later in Section 2.3. For now, it suffices to know that D-optimal designs can be defined for our problem.

### 1.3 Measurement Clusterization

Surprisingly, A- and D-optimal designs for inverse problems have been observed to yield remarkably similar measurements in certain cases [14, 31, 15, 44, 29]. This phenomenon

---

<sup>1</sup>Code generating these movies is located in module `movies.py` in the accompanying [repository](#).

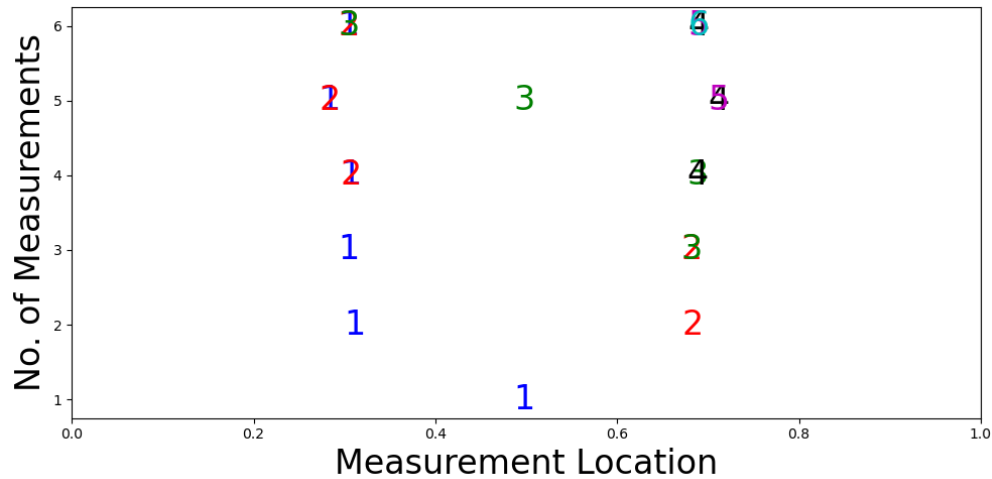


Figure 1: Measurement clusterization in D-optimal designs for the inverse problem of the 1D heat equation. Measurement locations were chosen according to the Bayesian D-optimality criterion of Theorem 2.1. Measurement locations are plotted over the computational domain  $\Omega = [0, 1]$  (x-axis), for varying numbers of measurements (y-axis). The colored numbers are measurement indices, plotted for visual clarity. Measurement clusterization already occurs for three measurements: the second measurement (red) is overlaid on the third (green). For five measurements, first (blue) and second (red) measurements are clustered, as well as the fourth (black) and the fifth (magenta).

is illustrated for our toy inverse problem in Fig. 1, where D-optimal measurement locations are shown for different numbers of measurements. Notably, for six measurements, a D-optimal design yields two sets of measurements that are identical. Following [44], we refer to this intriguing phenomenon as *measurement clusterization*. We consider a design to be *clustered* when two or more of its constituent measurements are identical.

Clusterization should not be confused with replication. Replication requires that the experimentalist executes multiple trials under circumstances that are *nominally identical* [28, Section 1.2.4]. Replication is commonly viewed as a beneficial and even necessary aspect of optimal experimental design [16, 28, 37]. For example, [16], suggested repeating his famous milk and tea experiment in order "to be able to demonstrate the predominance of correct classifications in spite of occasional errors". Unfortunately, in the experiments we consider, replication is impossible. For example, in the MRI problem, we cannot generate an individual nominally identical to the one we wish to scan.

Similarly to a design implementing replication, a clustered design reduces the signal-to-noise ratio of the repeated measurements [43]. The difference is that a clustered design takes repeated measurements at the expense of other quantities not measured at all. For example, consider an experiment measuring the effect of rainfall on grass growth [13]. The experiment involved four rainfall manipulation "treatments" (i.e. simulating

different timing and quantity of rainfall), each replicated three times over different plots of land. Indeed, it seems reasonable for researchers to replicate the phenomenon they are trying to study. A clustered design in such an experiment would imply the researchers should take a repeated measurement *on the same plot*, at the expense of measuring grass growth in other plots!

As another example illustrating the differences between replication and clusterization, consider an experiment involving a chemical reaction conducted at different temperatures. An investigator may choose to repeat the experiment at  $10^{\circ}\text{C}$  and  $30^{\circ}\text{C}$ , giving rise to *replication*. Within a single experiment, the investigator may also sample the concentrations of the reagents through the course of the experiment. Simultaneous sampling (within a single experiment) gives rise to *clusterization*. While replication is intuitively sensible for this chemical experiment, clusterization is not.

To conclude our short discussion on replication vs. clusterization: these are fundamentally different concepts and even though replication is quite intuitive, it is inapplicable to the inverse problems we consider in this manuscript.

Measurement clusterization is generally considered undesirable [14, 31, 15, 44, 29]. It is counterintuitive for a so-called "optimal" design to prioritize marginally improving accuracy in a small region over taking measurements in unexplored regions of the computational domain, where they could significantly reduce uncertainty.

The issue with clusterization is evident in Fig. 1, where most clustered designs shown place little to no measurement weight in the center of the domain, where prior uncertainty is largest. It seems as though a clustered design assumes that focusing measurement efforts on a small subset of the domain can somehow yield information about the entire domain. Intuitively, this is an unreasonable assumption, albeit it holds for *linear* models.

The view that clusterization is undesirable prompted the exploration of various remedies to address this issue. One approach involves merging close measurements [15]; however, this strategy merely overlooks the phenomenon of measurement clusterization. An alternative solution lies in *clusterization-free designs*, where measurement locations are deliberately chosen to be distant from one another. This can be achieved by imposing distance constraints between measurements or by introducing correlated errors that account for both observation error and model misspecification [44]. For instance, in the context of time-series analysis for pharmacokinetic experiments, measurement clusterization can be mitigated by incorporating the modeling of auto-correlation time within the noise terms [31].

In spatial problems involving choice of measurements within a domain  $\Omega \subseteq \mathbb{R}^d$ ,  $d = 1, 2, 3$ , many researchers circumvent the problem of measurement clusterization by restricting measurements to a coarse grid in  $\Omega$  [24, 4, 6, 2, 3, 5, 9]. This approach incurs a significant computational cost as it requires solving a difficult combinatorial optimization problem for measurement locations over a discrete set. The combinatorial optimization problem is usually relaxed by first assigning optimal measurement weights in  $\mathbb{R}_+$  to the potential measurement locations. Some researchers incorporate a sparsifying  $\ell_1$  penalty term into the design criterion, which is subsequently thresholded to achieve

the desired binary design over the coarse grid [17]. Others progressively relax the  $\ell_1$  penalty to an  $\ell_0$  penalty via a continuation method [3, 2]. Others cast the problem of finding optimal measurement weights as a stochastic optimization problem [7]. All of the aforementioned methods may indeed find a binary optimal design restricted to a given coarse grid. However, none addresses one fundamental issue: the restriction of measurement locations to a coarse grid in  $\Omega$  fundamentally changes the optimal design problem and thus results in a sub-optimal design.

Avoiding measurement clusterization is a pragmatic approach: intuitively, researchers recognize that measurement clusterization is undesirable, even though the underlying reasons may not be fully clear. Consequently, they strive to prevent it and devise various methodologies to avoid it. Yet each and every one of these methodologies achieves its objective by imposing restrictions on measurement locations, thereby fundamentally altering the optimal design problem. To the best of my knowledge, no previous study has tried to address some seemingly simple yet fundamental questions: Why does imposing correlations between observations alleviate measurement clusterization? Is measurement clusterization a generic phenomenon? And, most importantly: Why does measurement clusterization occur?

## 1.4 Contribution

The primary objective of this study is to provide a deep understanding of measurement clusterization by addressing the aforementioned questions. Our focus centers around investigating the Bayesian D-optimality criterion. We conduct an analysis of Bayesian D-optimal designs within the context of linear inverse problems over Hilbert spaces and study two inverse problems: (a) In Sections 2 and 3 we propose a novel generic model for an inverse problem where D-optimality maintains analytical tractability and D-optimal designs are identified via Lagrange multipliers. This analytical framework facilitates the exploration of the questions posed at the end of the previous paragraph. We also study (b) the inverse problem of the 1D heat equation from Section 1.2 above. Investigating both inverse problems allows us to answer the questions posed in the previous section:

1. **Is measurement clusterization a generic phenomenon?** We give two complementing answers to this question. First, from a theoretical perspective, we show that clusterization mainly depends on how quickly the eigenvalues of the prior covariance in observation space decay. See Section 5 — particularly, Theorem 5.7 and the discussion following it. Furthermore, in Section 6.1 we show results of numerical experiments, where simulations of our model give rise to D-optimal designs that exhibit clusterization with high probability. Thus, given the genericity of our model, we expect measurement clusterization to be a generic and ubiquitous phenomenon.
2. **Why does imposing correlations between observations alleviate measurement clusterization?** In Section 4, we rigorously demonstrate the role of model error in mitigating clusterization, thereby corroborating earlier observations

made by various researchers. Specifically, our proof shows that identical measurements result in no gain in design criterion when observation error amplitude tends to zero. Moreover, in Section 6.2, we show that an error term corresponding to correlations between measurements mitigates clusterization in the inverse problem of the 1D heat equation.

3. **Why does measurement clusterization occur?** In Sections 5.1 we give two compelling answers to this question by (i) transporting insights we gain from our generic model to the inverse problem of the 1D heat equation, and (ii) connecting measurement clusterization to Carathéodory’s Theorem.

Our analysis for the heat equation relies on conclusions from our generic model. In particular, Theorem 5.7 reveals that a D-optimal design focuses on a select set of prior eigenvectors, i.e. those with the largest eigenvalues in the prior covariance spectrum. In practical scenarios, the number of locations where (a) all relevant prior eigenvectors are significantly large, and (b) other eigenvectors are close to zero, is limited. Consequently, the clusterization of measurements arises as a natural consequence of the pigeonhole principle, as there are more measurements available than there are locations satisfying conditions (a) and (b).

The connection to Carathéodory’s Theorem also builds on the focus of measurement effort to the abovementioned select set of prior eigenvectors. This allows us to move from an infinite-dimensional setting to finite dimensions, where the conditions of Carathéodory’s Theorem hold. We conclude that a D-optimal design arises by weighting a small number of measurements. If the number of allowed measurements is larger than the small number dictated by Carathéodory’s Theorem, we have excessive weight on some measurements, which can be interpreted as clusterization.

### Implications

Our answer to Question 1 implies that encountering clusterization could be expected in many different problems across many different scientific fields. Researchers that encounter clusterization should not be surprised or wary. In Our answer to Question 3, we explain what our view of the cause of clusterization is. It appears, the cause is generic: a D-optimal design reduces uncertainty for a select set of prior covariance eigenvectors — those with the most prior uncertainty, i.e. those the practitioner cares about the most!

A further implication of the analysis we present is that clusterization can serve as an evidence to the number of relevant eigenvectors in the problem. These eigenvectors correspond to the relevant degrees of freedom in the problem. Thus, clusterization tells us that we might be able to reduce the complexity of a computational model, e.g. by dropping discretization points.

One potential cause of clusterization is our choice of prior. Gaussian priors, coupled with a Gaussian likelihood and a linear forward problem give rise to a closed form solution for the posterior via conjugacy. As we show in Section 6.1, such assumptions generically give rise to clusterization. While an assumption of a Gaussian likelihood



(i.e. independent Gaussian noise) is standard, and rooted in the central limit theorem, an assumption of Gaussian prior is merely a matter of convenience. Therefore, we advise any practitioner who encounters clusterization to replace their Gaussian priors with non-Gaussian priors instead [19, 20], as these are not only more realistic but also expected to mitigate clusterization.

Another potential cause of clusterization is linearization. While in a real applications the model is not necessarily linear, some authors consider a linearized version of their model when seeking optimal designs [14, 29]. Our analysis then shows that the linearity of the forward problem is also an important ingredient in giving rise to clustered designs. Therefore, our advice to practitioners is to avoid linearization, and find D-optimal designs via other methods, e.g. the sampling method of [36].

Given the above discussion, it is our belief that the methods suggested by other authors to avoid clusterization are merely overlooking the problem. We do not view clustered designs as inherently bad on their own. Rather, we suggest that if a clustered design arises, a practitioner should revisit their modeling choices — specifically, their choice of prior and model linearization. If the practitioner is confident in their analysis, then clustered designs should be avoided only to the extent necessitated by the physical measuring apparatus.

Clusterization in D-optimal designs raises the question of whether D-optimal designs should be pursued at all. While other authors have established convergence results for decaying measurement error [23], space-filling measurements [42] and randomly sampled designs [30], their results do not hold for D-optimal designs. Luckily, we can expect convergence from D-optimal designs (including clustered designs) in the following sense: the posterior uncertainty ellipsoid will contract to zero along each one of its eigenvectors. See Section 5.1 for a precise statement and a proof based on Theorem 5.7 — the main theorem of this manuscript.

## Other Contributions

In Theorem 5.7, we also show that D-optimal designs are best understood in the space of *observations*. This is in accordance with previous work by [24], who showed that A-optimal designs are best constructed in the space of observations.

In the process of proving Theorem 5.7 we prove and generalize several lemmas. Among those, is Lemma 5.6, which is (to the the best of my knowledge) novel: We decompose a symmetric positive definite matrix  $M \in \mathbb{R}^{k \times k}$  with  $\text{tr } M = m \in \mathbb{N}$  as  $M = AA^t$ , where  $A \in \mathbb{R}^{k \times m}$  has unit norm columns.

## 1.5 Limitations

The main limitation of this study is that our generic model does not correspond to any specific real-life problem. Specifically, in its current form, our model does not allow point evaluations. Thus, while our model is generic enough to be analytically tractable, one may argue that our model is too far removed from any real application. To these

claims I would answer that scientists have a long history of studying models that are bare-bones simplifications of real systems, e.g. the Ising model [11], the Lorenz system [8], the Lotka-Volterra equations [26], the Carnot engine [22] and many others.

## 2 Preliminaries and Notation

Here we present the basics of Bayesian inverse problems over Hilbert spaces. Since we are ultimately interested in inferring a function over some domain, we will keep in mind that these Hilbert spaces should really be thought of as function spaces, utilizing a setup similar to [23]. A deeper treatment of the foundations for inverse problems over function spaces can be found in [40].

### 2.1 Forward Problems

In this section we give definitions and notations for forward problems, which are an essential part of the inverse problems we discuss later. Consider a "parameter space"  $\mathcal{H}_p$  and an "observation space"  $\mathcal{H}_o$  — both separable Hilbert spaces (the subscripts p and o are for "parameter" and "observation", respectively). The parameter space includes the quantity we seek to infer; in the inverse problem of the heat equation, the parameter space  $\mathcal{H}_p$  is where the initial condition lives. The observation space  $\mathcal{H}_o$ , on the other hand, is the space from which we take measurements; in the example of the heat equation,  $u(\cdot, T) \in \mathcal{H}_o$ .

The connection between parameter and observation spaces is made by the *forward operator*  $\mathcal{F} : \mathcal{H}_p \rightarrow \mathcal{H}_o$ . We assume the forward operator  $\mathcal{F}$  is linear. In the inverse problem of the 1D heat equation, the forward operator is determined by the time evolution of the 1D heat equation (2a) and (2b), so  $u(\cdot, T) = \mathcal{F}u_0$ .

Measurements are taken via a linear *measurement operator*  $\mathcal{O}$ , which is the concatenation of linear functionals  $\mathbf{o}_1, \dots, \mathbf{o}_m$  we call *measurements*:

$$\mathcal{O}u = (\mathbf{o}_1(u), \dots, \mathbf{o}_m(u))^t \in \mathbb{R}^m, \quad u \in \mathcal{H}_o.$$

Thus,  $\mathcal{O} \in (\mathcal{H}_o^*)^m$ , where  $m$  is the number of measurements taken<sup>2</sup>.

Data is acquired via noisy observations, and we consider two types of error terms: Spatially correlated model error  $\varepsilon' \sim \mathcal{N}(0, \Gamma_{\text{model}})$  with  $\Gamma_{\text{model}}$  a covariance operator; and observation error denoted  $\varepsilon \sim \mathcal{N}(0, \sigma^2 I_m)$ , with  $I_m \in \mathbb{R}^{m \times m}$  the identity. Both error terms and the prior (see Section 2.2 below) are assumed independent of each other. Thus, data is acquired via

$$\mathbf{d} := \mathcal{O}(\mathcal{F}\mathbf{m} + \varepsilon') + \varepsilon = \mathcal{O}\mathcal{F}\mathbf{m} + \mathcal{O}\varepsilon' + \varepsilon. \quad (4)$$

---

<sup>2</sup>The alert reader will likely ask how do we reconcile point measurements  $\delta_x$  as suggested by the formulation of the 1D heat equation with working in Hilbert spaces. We don't. We follow standard practice in the literature and restrict our analysis to Hilbert spaces. We can satisfy ourselves with the fact that point evaluations could be approximated in a standard Hilbert space like  $L^2(\Omega)$ .

It is easy to verify that  $\mathcal{O}\varepsilon' + \varepsilon \in \mathbb{R}^m$  is a centered Gaussian random vector with covariance matrix

$$\Sigma(\mathcal{O}) := \mathbb{E}[(\mathcal{O}\varepsilon' + \varepsilon)(\mathcal{O}\varepsilon' + \varepsilon)^t] = \mathcal{O}\Gamma_{\text{model}}\mathcal{O}^* + \sigma^2 I_m, \quad (5)$$

where

$$[\mathcal{O}\Gamma_{\text{model}}\mathcal{O}^*]_{ij} = e_i^t \mathcal{O}\Gamma_{\text{model}}\mathcal{O}^* e_j = \mathbf{o}_i(\Gamma_{\text{model}}\mathbf{o}_j). \quad (6)$$

Taking  $\Gamma_{\text{model}} = 0$  is a common practice [41, 21, 45] and then  $\Sigma = \sigma^2 I_m$  is a scalar matrix which does not depend on  $\mathcal{O}$ .

## 2.2 Bayesian Linear Inverse Problems

In the previous section, we saw how a parameter  $u \in \mathcal{H}_p$  is transported to the observation space via the forward operator  $\mathcal{F}u \in \mathcal{H}_o$ , how observations are generated from a parameter via  $\mathcal{O}\mathcal{F}u$  and how observations and noise give rise to data  $\mathbf{d}$ . It is time to formulate the process of inferring the parameter as a Bayesian inverse problem. We have already defined the Gaussian likelihood in the previous section, and now we will define the prior.

We take a Gaussian prior  $\mathbf{m} \sim \mu_{\text{pr}} = \mathcal{N}(\mathbf{m}_{\text{pr}}, \Gamma_{\text{pr}})$  with some appropriate covariance operator  $\Gamma_{\text{pr}}$  on  $\mathcal{H}_p$  [40]. For example, for the inverse problem of the 1D heat equation we chose  $\Gamma_{\text{pr}} = (-\Delta)^{-1}$ , as described in Section 1.2. Note that  $\mathcal{F}\Gamma_{\text{pr}}\mathcal{F}^*$  is the prior covariance in  $\mathcal{H}_o$  [40], and as such is assumed invertible — an assumption which we will use later (if  $\mathcal{F}$  has a nontrivial kernel we utilize Occam's Razor and ignore said kernel altogether).

Since  $\mathcal{F}$  is linear and  $\mu_{\text{pr}}$  is Gaussian — the posterior  $\mu_{\text{post}}$  is Gaussian as well. We do not utilize the posterior mean in this study, but the posterior covariance operator  $\Gamma_{\text{post}}$  is given by the known formula [40]:

$$\Gamma_{\text{post}} = (\Gamma_{\text{pr}}^{-1} + \mathcal{F}^*\mathcal{O}^*\Sigma^{-1}\mathcal{O}\mathcal{F})^{-1}. \quad (7)$$

## 2.3 Bayesian D-Optimal Designs

A Bayesian D-optimal design maximizes the expected KL divergence between posterior  $\mu_{\text{post}}$  and prior measures  $\mu_{\text{pr}}$ . For arbitrary posterior and prior measures, the KL divergence is defined, analogously to eq. (1), via the Radon-Nikodym derivative:

$$D_{KL}(\mu_{\text{post}}||\mu_{\text{pr}}) = \int \log \frac{d\mu_{\text{post}}}{d\mu_{\text{pr}}}(\mathbf{m}) d\mu_{\text{post}}(\mathbf{m}).$$

The study of D-optimal designs for Bayesian linear inverse problems in infinite dimensions was pioneered by [1, 5]. The main result we will make use of is summarized (in our notation) below:

**Theorem 2.1** (Alexanderian, Gloor, Ghattas [1]). *Let  $\mu_{\text{pr}} = \mathcal{N}(\mathbf{m}_{\text{pr}}, \Gamma_{\text{pr}})$  be a Gaussian prior on  $\mathcal{H}_p$  and let  $\mu_{\text{post}} = \mathcal{N}(\mathbf{m}_{\text{post}}, \Gamma_{\text{post}})$  the posterior measure on  $\mathcal{H}_p$  for the Bayesian linear inverse problem  $\mathbf{d} = \mathcal{O}\mathcal{F}\mathbf{m} + \mathcal{O}\varepsilon' + \varepsilon$  discussed above. Then*

$$\begin{aligned} \Psi(\mathcal{O}) &:= \mathbb{E}_{\mathbf{d}} [D_{KL}(\mu_{\text{post}} \parallel \mu_{\text{pr}})] \\ &= \frac{1}{2} \log \det(I + \Gamma_{\text{pr}}^{1/2} \mathcal{F}^* \mathcal{O}^* \Sigma^{-1} \mathcal{O} \mathcal{F} \Gamma_{\text{pr}}^{1/2}). \end{aligned} \quad (8)$$

In [1, 5], results are stated for  $\Sigma = I$  (implied by  $\Gamma_{\text{model}} = 0, \sigma^2 = 1$ ), but these results also hold for more general covariance matrices [1, p. 681].

**Definition 2.2.** We say  $\mathcal{D}$  is *D-optimal* if  $\mathcal{D} = \arg \max_{\mathcal{O}} \Psi(\mathcal{O})$ , where entries of  $\mathcal{O} \in (\mathcal{H}_o^*)^m$  are constrained to some allowed set of measurements in  $\mathcal{H}_o^*$ .

Intuition for Theorem 2.1 can be gained by recalling from Section 1.1 that for a Bayesian linear model in finite dimensions, with Gaussian prior and Gaussian noise, a D-optimal design minimizes the determinant of the posterior covariance matrix. Theorem 2.1 and Definition 2.2 carry a similar intuition:

$$\begin{aligned} \Psi(\mathcal{O}) &= \frac{1}{2} \log \det(I + \Gamma_{\text{pr}}^{1/2} \mathcal{F}^* \mathcal{O}^* \Sigma^{-1} \mathcal{O} \mathcal{F} \Gamma_{\text{pr}}^{1/2}) \text{ by (8)} \\ &= \frac{1}{2} \log \det \left( \Gamma_{\text{pr}} (\Gamma_{\text{pr}}^{-1} + \mathcal{F}^* \mathcal{O}^* \Sigma^{-1} \mathcal{O} \mathcal{F}) \right) \\ &= \frac{1}{2} \log \det \Gamma_{\text{pr}} \Gamma_{\text{post}}^{-1} \text{ by (7)}. \end{aligned}$$

We think of  $\Gamma_{\text{pr}}$  as constant, in the sense that  $\Gamma_{\text{pr}}$  does not depend on data  $\mathbf{d}$ . Thus, a D-optimal design minimizes a quantity analogous to the posterior covariance determinant, similarly to the finite-dimensional case.

### 3 The Constrained Optimization Problem of D-Optimal Design

We seek a formulation of the D-optimal design problem via Lagrange multipliers. We first find the gradient of  $\Psi$ , then we suggest unit-norm constraints on  $\mathcal{O}$  and find their gradients. Results of this section are summarized in Theorem 3.5. First, recall that:

**Definition 3.1.** Let  $F$  a real valued function of  $\mathcal{O}$ . The first variation of  $F$  at  $\mathcal{O}$  in the direction  $V$  is:

$$\delta F(\mathcal{O})V := \left. \frac{d}{d\tau} \right|_{\tau=0} F(\mathcal{O} + \tau V).$$

Moreover, if

$$\delta F(\mathcal{O})V = \text{tr} \{ \nabla F(\mathcal{O})V \},$$

then we call  $\nabla F(\mathcal{O})$  the gradient of  $F$  at  $\mathcal{O}$ .

**Proposition 3.2.** *The gradient of the D-optimality objective  $\Psi$  is*

$$\nabla\Psi(\mathcal{O}) = (I - \Gamma_{\text{model}}\mathcal{O}^*\Sigma^{-1}\mathcal{O})\mathcal{F}\Gamma_{\text{post}}\mathcal{F}^*\mathcal{O}^*\Sigma^{-1}$$

The proof amounts to calculating the variational derivative of  $\Psi$  at  $\mathcal{O}$  for any direction  $V$  (by Definition 3.1) and is delegated to the Supplementary.

### 3.1 Unit norm constraints and their gradient

In a real-life optimal design problem we cannot choose any measurement operator  $\mathcal{O} \in (\mathcal{H}_o^*)^m$ . In order to facilitate analysis, we seek reasonable constraints on  $\mathcal{O}$  for which finding a D-optimal design is analytically tractable. The following proposition will guide us in finding such constraints.

**Proposition 3.3.** *Let  $\mathcal{O} = (\mathbf{o}_1, \dots, \mathbf{o}_m)^t$ ,  $j \in \{1, \dots, m\}$ ,  $\sigma^2 > 0$  and  $|\zeta| > 1$ . Then  $\Psi(\mathcal{O})$  increases if we use  $\zeta\mathbf{o}_j$  in  $\mathcal{O}$  instead of  $\mathbf{o}_j$ .*

*Proof.* Fix  $j = 1, \dots, m$  and take  $V := e_j e_j^t \mathcal{O}$ . For  $u \in \mathcal{H}_o$ :

$$Vu = e_j e_j^t (\mathbf{o}_1(u), \dots, \mathbf{o}_m(u))^t = e_j \mathbf{o}_j(u) = (0, \dots, 0, \mathbf{o}_j(u), 0, \dots, 0)^t.$$

We now calculate the variation of  $\Psi$  at  $\mathcal{O}$  in the direction of  $V$ . Denote  $\mathcal{G} := \mathcal{F}\Gamma_{\text{post}}\mathcal{F}^*$ . From Proposition 3.2:

$$\begin{aligned} \delta\Psi(\mathcal{O})V &= \text{tr} \{V(I - \Gamma_{\text{model}}\mathcal{O}^*\Sigma^{-1}\mathcal{O})\mathcal{G}\mathcal{O}^*\Sigma^{-1}\} \\ &= \text{tr} \{e_j e_j^t \mathcal{O}(I - \Gamma_{\text{model}}\mathcal{O}^*\Sigma^{-1}\mathcal{O})\mathcal{G}\mathcal{O}^*\Sigma^{-1}\} \\ &= e_j^t \mathcal{O}(I - \Gamma_{\text{model}}\mathcal{O}^*\Sigma^{-1}\mathcal{O})\mathcal{G}\mathcal{O}^*\Sigma^{-1} e_j \\ &= e_j^t (I - \mathcal{O}\Gamma_{\text{model}}\mathcal{O}^*\Sigma^{-1})\mathcal{O}\mathcal{G}\mathcal{O}^*\Sigma^{-1} e_j \\ &= e_j^t (\Sigma - \mathcal{O}\Gamma_{\text{model}}\mathcal{O}^*)\Sigma^{-1}\mathcal{O}\mathcal{G}\mathcal{O}^*\Sigma^{-1} e_j \\ &= \sigma^2 e_j^t \Sigma^{-1}\mathcal{O}\mathcal{G}\mathcal{O}^*\Sigma^{-1} e_j \text{ by (5)} \\ &= \sigma^2 e_j^t \Sigma^{-1}\mathcal{O}\mathcal{F}\Gamma_{\text{post}}\mathcal{F}^*\mathcal{O}^*\Sigma^{-1} e_j. \end{aligned}$$

Since  $\Gamma_{\text{post}}$  is positive definite, we conclude that  $\delta\Psi(\mathcal{O})V > 0$ . This means that increasing the magnitude of the  $j^{\text{th}}$  measurement functional increases  $\Psi(\mathcal{O})$ .  $\square$

Proposition 3.3 implies that it is a good idea to bound the norm of measurements. If, for example, we can take measurements in  $\text{span}\{\mathbf{o}\}$  for some  $\mathbf{o} \neq 0$ , then the D-optimality criterion is unbounded, so a D-optimal design does not exist. In contrast, in any real-life problem where sensors are concerned, the norm of measurements recorded by sensors is always one<sup>3</sup>:

<sup>3</sup>Again, our analysis does not directly apply to point evaluations. We just utilize point evaluations for motivation. We can approximate point evaluations by e.g. elements in  $\mathcal{H}_o^*$  as long as  $\mathcal{H}_o$  is a function space, e.g.  $L^2(\Omega)$ . In this case, for a fixed approximation of  $\delta$  the norm of the corresponding functional is a constant  $\neq 1$ .

$$\|\delta_{\mathbf{x}}\| = \sup_{0 \neq u \in C(\Omega)} \frac{|\int_{\Omega} u(\mathbf{y}) \delta_{\mathbf{x}}(\mathbf{y}) d\mathbf{y}|}{\sup |u|} = \sup_{0 \neq u \in C(\Omega)} \frac{|u(\mathbf{x})|}{\sup |u|} = 1, \forall \mathbf{x} \in \Omega. \quad (9)$$

Thus, it is reasonable to consider measurements with unit  $\mathcal{H}_o^*$  norm. We can write the unit norm constraints as a series of  $m$  equality constraints (one for each measurement) on  $\mathcal{O}$ . We define them and find their gradients in Proposition 3.4 below, whose proof is straightforward and delegated to the Supplementary:

**Proposition 3.4.** *Let*

$$\phi_j(\mathcal{O}) := \frac{1}{2} \|\mathcal{O}^* e_j\|_{\mathcal{H}_p}^2 - \frac{1}{2} = 0, \quad j = 1, \dots, m.$$

*Then*

$$\nabla \phi_j(\mathcal{O}) = \mathcal{O}^* e_j e_j^t.$$

### 3.2 Necessary conditions for D-optimality

We find necessary first-order conditions for D-optimality via Lagrange multipliers:

$$\nabla \Psi(\mathcal{O}) = \sum_{j=1}^m \xi_j \nabla \phi_j(\mathcal{O}) \quad (10)$$

$$\phi_j(\mathcal{O}) = 0, j = 1, \dots, m. \quad (11)$$

We now substitute the gradients calculated in Propositions 3.2 and 3.4 into eq. (10):

$$(I - \Gamma_{\text{model}} \mathcal{O}^* \Sigma^{-1} \mathcal{O}) \mathcal{F} \Gamma_{\text{post}} \mathcal{F}^* \mathcal{O}^* \Sigma^{-1} = \sum_{j=1}^m \xi_j \mathcal{O}^* e_j e_j^t = (\xi_1 \mathbf{o}_1, \dots, \xi_m \mathbf{o}_m). \quad (12)$$

Letting  $\Xi := \text{diag}(\xi_j)$ , we can write (12) and (11) more compactly as:

**Theorem 3.5** (Necessary conditions for D-Optimality). *Let:*

$$\mathcal{D} = \arg \max_{\|\mathbf{o}_j\|=1, j=1, \dots, m} \Psi(\mathcal{O}).$$

*Then:*

$$(I - \Gamma_{\text{model}} \mathcal{D}^* \Sigma^{-1} \mathcal{D}) \mathcal{F} \Gamma_{\text{post}} \mathcal{F}^* \mathcal{D}^* \Sigma^{-1} = \mathcal{D}^* \Xi,$$

where  $\Xi \in \mathbb{R}^{m \times m}$  is diagonal.

## 4 Answer to Question 2: Model error mitigates clusterization

We now show that if  $\Gamma_{\text{model}} \neq 0$  clusterization will not occur. It is known that including a model error term mitigates the clusterization phenomenon [44], and here we prove this rigorously. Let  $\mathcal{O} = (\mathbf{o}_1, \dots, \mathbf{o}_m)^t$  and  $\hat{\mathcal{O}} := (\mathbf{o}_1, \dots, \mathbf{o}_{m-1})^t$ . Denote  $\hat{\Sigma} := \Sigma(\hat{\mathcal{O}})$  and  $\widehat{\Gamma}_{\text{post}}$  the posterior covariance that arises when  $\hat{\mathcal{O}}$  is utilized as a measurement operator.

**Proposition 4.1** (Increase due to a measurement). *Let  $\mathcal{O} = (\mathbf{o}_1, \dots, \mathbf{o}_m)^t$  and  $\hat{\mathcal{O}} := (\mathbf{o}_1, \dots, \mathbf{o}_{m-1})^t$ . Then*

$$\Psi(\mathcal{O}) - \Psi(\hat{\mathcal{O}}) = \frac{1}{2} \log \left( 1 + \frac{\langle \mathcal{F} \widehat{\Gamma}_{\text{post}} \mathcal{F}^* (\hat{\mathcal{O}}^* \hat{\Sigma}^{-1} \Gamma_{\text{model}} - I) \mathbf{o}_m, (\hat{\mathcal{O}}^* \hat{\Sigma}^{-1} \Gamma_{\text{model}} - I) \mathbf{o}_m \rangle}{\sigma^2 + \mathbf{o}_m \Gamma_{\text{model}} \mathbf{o}_m - \mathbf{o}_m \Gamma_{\text{model}} \hat{\mathcal{O}}^* \hat{\Sigma}^{-1} \hat{\mathcal{O}} \Gamma_{\text{model}} \mathbf{o}_m} \right). \quad (13)$$

The proof is long and tedious, and is delegated to the Supplementary.

**Corollary 4.2.** *If  $\mathbf{o}_m = \mathbf{o}_j$  for some  $1 \leq j \leq m-1$ , then*

$$\Psi(\mathcal{O}) - \Psi(\hat{\mathcal{O}}) = \log \left( 1 + \frac{\sigma^2 \langle \mathcal{F} \widehat{\Gamma}_{\text{post}} \mathcal{F}^* \hat{\mathcal{O}}^* \hat{\Sigma}^{-1} e_j, \hat{\mathcal{O}}^* \hat{\Sigma}^{-1} e_j \rangle}{2 - \sigma^2 e_j^t \hat{\Sigma}^{-1} e_j} \right),$$

where  $e_j \in \mathbb{R}^{m-1}$  is the  $j^{\text{th}}$  standard unit vector.

*Proof.* Denote  $A := \mathcal{O} \Gamma_{\text{model}} \mathcal{O}^*$  and  $v_j$  the  $j^{\text{th}}$  column of  $A$ . Note that  $v_j = \hat{\mathcal{O}} \Gamma_{\text{model}} \mathbf{o}_m$ , since  $(\hat{\mathcal{O}} \Gamma_{\text{model}} \hat{\mathcal{O}}^*)_{ij} = \mathbf{o}_i (\Gamma_{\text{model}} \mathbf{o}_j)$ , as explained in the paragraph preceding eq. (6). We can now verify that

$$\hat{\Sigma}^{-1} \hat{\mathcal{O}} \Gamma_{\text{model}} \mathbf{o}_m = \hat{\Sigma}^{-1} v_j = (A + \sigma^2 I_{m-1})^{-1} v_j = e_j - \sigma^2 \hat{\Sigma}^{-1} e_j. \quad (14)$$

Using (14):

$$\begin{aligned} \mathbf{o}_m \Gamma_{\text{model}} \hat{\mathcal{O}}^* \hat{\Sigma}^{-1} \hat{\mathcal{O}} \Gamma_{\text{model}} \mathbf{o}_m &= \mathbf{o}_m \Gamma_{\text{model}} \hat{\mathcal{O}}^* (e_j - \sigma^2 \hat{\Sigma}^{-1} e_j) \\ &= \mathbf{o}_m \Gamma_{\text{model}} \mathbf{o}_j - \sigma^2 \mathbf{o}_m \Gamma_{\text{model}} \hat{\mathcal{O}}^* \hat{\Sigma}^{-1} e_j \\ &= \mathbf{o}_m \Gamma_{\text{model}} \mathbf{o}_j - \sigma^2 (e_j - \sigma^2 \hat{\Sigma}^{-1} e_j)^t e_j \\ &= \mathbf{o}_m \Gamma_{\text{model}} \mathbf{o}_m - \sigma^2 + \sigma^4 e_j^t \hat{\Sigma}^{-1} e_j. \end{aligned} \quad (15)$$

We use (14) to simplify the numerator in (13):

$$\begin{aligned} (\hat{\mathcal{O}}^* \hat{\Sigma}^{-1} \hat{\mathcal{O}} \Gamma_{\text{model}} - I) \mathbf{o}_m &= \hat{\mathcal{O}}^* \hat{\Sigma}^{-1} \hat{\mathcal{O}} \Gamma_{\text{model}} \mathbf{o}_m - \mathbf{o}_m \\ &= \hat{\mathcal{O}}^* (e_j - \sigma^2 \hat{\Sigma}^{-1} e_j) - \mathbf{o}_j \\ &= -\sigma^2 \hat{\mathcal{O}}^* \hat{\Sigma}^{-1} e_j. \end{aligned} \quad (16)$$

Now, we substitute (16) and (15) to the numerator and denominator of (13):

$$\begin{aligned}
\Psi(\mathcal{O}) - \Psi(\widehat{\mathcal{O}}) &= \log \left( 1 + \frac{\langle \widehat{\mathcal{F}}\widehat{\Gamma}_{\text{post}}\mathcal{F}^*(\widehat{\mathcal{O}}^*\widehat{\Sigma}^{-1}\Gamma_{\text{model}} - I)\mathbf{o}_m, (\widehat{\mathcal{O}}^*\widehat{\Sigma}^{-1}\Gamma_{\text{model}} - I)\mathbf{o}_m \rangle}{\sigma^2 + \mathbf{o}_m\Gamma_{\text{model}}\mathbf{o}_m - \mathbf{o}_m\Gamma_{\text{model}}\widehat{\mathcal{O}}^*\widehat{\Sigma}^{-1}\widehat{\mathcal{O}}\Gamma_{\text{model}}\mathbf{o}_m} \right) \\
&= \log \left( 1 + \frac{\sigma^4 \langle \widehat{\mathcal{F}}\widehat{\Gamma}_{\text{post}}\mathcal{F}^*\widehat{\mathcal{O}}^*\widehat{\Sigma}^{-1}e_j, \widehat{\mathcal{O}}^*\widehat{\Sigma}^{-1}e_j \rangle}{2\sigma^2 - \sigma^4 e_j^t \widehat{\Sigma}^{-1} e_j} \right) \\
&= \log \left( 1 + \frac{\sigma^2 \langle \widehat{\mathcal{F}}\widehat{\Gamma}_{\text{post}}\mathcal{F}^*\widehat{\mathcal{O}}^*\widehat{\Sigma}^{-1}e_j, \widehat{\mathcal{O}}^*\widehat{\Sigma}^{-1}e_j \rangle}{2 - \sigma^2 e_j^t \widehat{\Sigma}^{-1} e_j} \right).
\end{aligned}$$

□

Recall from (5) that  $\Sigma(\mathcal{O}) = \mathcal{O}\Gamma_{\text{model}}\mathcal{O}^* + \sigma^2 I$  and let  $u := \widehat{\mathcal{O}}^*\widehat{\Sigma}^{-1}e_j$ . Then

$$\begin{aligned}
\lim_{\sigma^2 \rightarrow 0} u &= \widehat{\mathcal{O}}^*(\widehat{\mathcal{O}}\Gamma_{\text{model}}\widehat{\mathcal{O}}^*)^{-1}e_j \\
\lim_{\sigma^2 \rightarrow 0} \widehat{\Gamma}_{\text{post}} &= (\Gamma_{\text{pr}}^{-1} + \mathcal{F}^*\widehat{\mathcal{O}}^*(\widehat{\mathcal{O}}\Gamma_{\text{model}}\widehat{\mathcal{O}}^*)^{-1}\widehat{\mathcal{O}}\mathcal{F})^{-1} \quad (\text{From (7)}).
\end{aligned}$$

Consequently,

$$\langle \widehat{\mathcal{F}}\widehat{\Gamma}_{\text{post}}\mathcal{F}^*\widehat{\mathcal{O}}^*\widehat{\Sigma}^{-1}e_j, \widehat{\mathcal{O}}^*\widehat{\Sigma}^{-1}e_j \rangle = \langle \widehat{\mathcal{F}}\widehat{\Gamma}_{\text{post}}\mathcal{F}^*u, u \rangle$$

is bounded, and

$$\lim_{\sigma^2 \rightarrow 0} \Psi(\mathcal{O}) - \Psi(\widehat{\mathcal{O}}) = 0.$$

We have shown that in the limit  $\sigma^2 \rightarrow 0$ , no increase in  $\Psi$  is gained by repeating a measurement. Thus, for vanishing noise levels, clustered designs cannot be D-optimal. For repeated measurements and  $\sigma^2 = 0$ ,  $\Sigma$  is not invertible and the posterior covariance is not defined in eq. (7). We can *define* the posterior in this case to equal the posterior when the repeated measurement is dropped, and under this definition, a repeated measurement trivially does not increase the design criterion when  $\sigma^2 = 0$ . Our results are stronger, since we show *continuity* in  $\sigma^2$ .

It is worth noting that by the nonnegativity of the KL divergence,  $\Psi$  cannot decrease upon adding measurements. However, we can construct examples where the posterior does not change upon taking a new measurement, e.g. if the prior variance vanishes on some eigenvector and a measurement is taken on said eigenvector. We do not expect a measurement to generate no information gain whatsoever in any realistic scenario, and ignore such pathologies.

In conclusion, for small observation error  $\sigma^2$  levels, measurement clusterization is mitigated by the presence of a non-zero model error  $\Gamma_{\text{model}}$  — answering Question 2 posed in the Introduction.



## 5 D-Optimal Designs Without Model Error

Our goal in this section is to prove Theorem 5.7 which characterizes D-optimal designs when  $\Gamma_{\text{model}} = 0$ . The necessary first-order condition for D-optimality of Theorem 3.5 for  $\Gamma_{\text{model}} = 0$  become:

$$\sigma^{-2} \mathcal{F} \Gamma_{\text{post}} \mathcal{F}^* \mathcal{O}^* = \mathcal{O}^* \Xi, \quad (17)$$

with  $\Xi$  diagonal. Equation (17) looks like an eigenvalue problem for the self-adjoint operator  $\sigma^{-2} \mathcal{F} \Gamma_{\text{post}} \mathcal{F}^*$ , where rows of  $\mathcal{O}$ , namely  $\mathbf{o}_j, j = 1, \dots, m$ , are eigenvectors. However,  $\Gamma_{\text{post}}$  depends on  $\mathcal{O}$ , so we refer to (17) as a *nonlinear* eigenvalue problem.

**Proposition 5.1.** *Assume  $\mathcal{F} \Gamma_{\text{pr}} \mathcal{F}^*$  is invertible. Then*

$$\mathcal{F}(\Gamma_{\text{pr}}^{-1} + \sigma^{-2} \mathcal{F}^* \mathcal{O}^* \mathcal{O} \mathcal{F})^{-1} \mathcal{F}^* = ((\mathcal{F} \Gamma_{\text{pr}} \mathcal{F}^*)^{-1} + \sigma^{-2} \mathcal{O}^* \mathcal{O})^{-1},$$

As we mentioned in Section 2.2,  $\mathcal{F} \Gamma_{\text{pr}} \mathcal{F}^*$  is the prior covariance in  $\mathcal{H}_o$  and could be safely assumed invertible. The proof of Proposition 5.1 is delegated to the Supplementary. It amounts to using Woodbury's matrix identity twice. The standard proof for Woodbury's matrix identity works for separable Hilbert spaces, as long as all terms are well defined. Unfortunately,  $\mathcal{O}^* \mathcal{O}$  is not invertible, so we utilize a regularization trick to force it to be.

**Lemma 5.2** (Simultaneous diagonalizability). *Let  $\mathcal{H}$  separable Hilbert space,  $C : \mathcal{H} \rightarrow \mathcal{H}$  self-adjoint and  $\mathbf{a}_1, \dots, \mathbf{a}_m \in \mathcal{H}$ . Denote  $\mathbf{a}^*$  the element  $\mathbf{a}$  acting as a linear functional. If*

$$(C + \sum_{j=1}^m \mathbf{a}_j \mathbf{a}_j^*) \mathbf{a}_l = \xi_l \mathbf{a}_l, \quad l = 1, \dots, m$$

then  $C$  and  $\sum_{j=1}^m \mathbf{a}_j \mathbf{a}_j^*$  are simultaneously diagonalizable.

The proof of Lemma 5.2 is delegated to the Supplementary.

**Proposition 5.3.** *Let  $\mathcal{O}$  satisfy the nonlinear eigenvalue problem (17). Then  $\mathcal{O}^* \mathcal{O}$  and  $\mathcal{F} \Gamma_{\text{pr}} \mathcal{F}^*$  are simultaneously diagonalizable.*

*Proof.*

$$\begin{aligned} \mathcal{O}^* \Xi &= \sigma^{-2} \mathcal{F} \Gamma_{\text{post}} \mathcal{F}^* \mathcal{O}^* \quad (\text{by (17)}) \\ &= \sigma^{-2} \mathcal{F} (\Gamma_{\text{pr}}^{-1} + \sigma^{-2} \mathcal{F}^* \mathcal{O}^* \mathcal{O} \mathcal{F})^{-1} \mathcal{F}^* \mathcal{O}^* \quad (\text{by (7)}) \\ &= \sigma^{-2} ((\mathcal{F} \Gamma_{\text{pr}} \mathcal{F}^*)^{-1} + \sigma^{-2} \mathcal{O}^* \mathcal{O})^{-1} \mathcal{O}^* \quad (\text{by Proposition 5.1}). \end{aligned} \quad (18)$$

Now take  $\mathbf{a}_j^* = \mathbf{o}_j$  and  $C := (\mathcal{F} \Gamma_{\text{pr}} \mathcal{F}^*)^{-1}$  and use Lemma 5.2. □

Since we made no assumption regarding the ordering of  $\{\lambda_i\}$ , we can denote the corresponding non-zero eigenvalues of  $\mathcal{O}^* \mathcal{O}$  by  $\{\eta_i\}_{i=1}^k$  and let  $\eta_i = 0$  for  $i \geq k + 1$ .

**Proposition 5.4.** *Let  $\mathcal{O}$  with  $m$  measurements satisfy the nonlinear eigenvalue problem (17). Let  $\{\eta_i\}_{i=1}^{\infty}$  eigenvalues of  $\mathcal{O}^*\mathcal{O}$  and  $\{\lambda_i\}_{i=1}^{\infty}$  the corresponding eigenvalues of  $\mathcal{F}\Gamma_{\text{pr}}\mathcal{F}^*$ . Let  $k := \text{rank } \mathcal{O}^*\mathcal{O}$ . Without loss of generality, let  $\eta_i > 0$  for  $i \leq k$  and  $\eta_i = 0$  for  $i > k$ . Then:*

1.  $k \leq m$  and  $\mathcal{O}^*\mathcal{O}$  has exactly  $k$  positive eigenvalues.

2.

$$\Psi(\mathcal{O}) = \frac{1}{2} \sum_{i=1}^k \log(1 + \sigma^{-2} \lambda_i \eta_i) = \frac{1}{2} \sum_{i=1}^m \log(1 + \sigma^{-2} \lambda_i \eta_i).$$

3. Furthermore, if  $\mathcal{O}$  is D-optimal,  $\eta_i > 0$  for eigenvectors corresponding to the  $k$  largest  $\lambda_i$ .

*Proof.* Part (1) is trivial. To see part (2) holds:

$$\begin{aligned} \Psi(\mathcal{O}) &= \frac{1}{2} \log \det \left( I + \sigma^{-2} \Gamma_{\text{pr}}^{1/2} \mathcal{F}^* \mathcal{O}^* \mathcal{O} \mathcal{F} \Gamma_{\text{pr}}^{1/2} \right) \\ &= \frac{1}{2} \log \det \left( I + \sigma^{-2} \mathcal{O}^* \mathcal{O} \mathcal{F} \Gamma_{\text{pr}} \mathcal{F}^* \right) \quad (\text{Sylvester's Determinant Theorem}) \\ &= \frac{1}{2} \log \prod_{i=1}^{\infty} (1 + \sigma^{-2} \lambda_i \eta_i) \quad (\text{Proposition 5.3}) \\ &= \frac{1}{2} \sum_{i=1}^k \log(1 + \sigma^{-2} \lambda_i \eta_i). \end{aligned} \tag{19}$$

Part (3) holds since log is increasing and  $\eta_i \geq 0$ . □

**Proposition 5.5.** *Let  $\Psi : \mathbb{R}^m \rightarrow \mathbb{R}$ ,  $\Psi(\eta) = \frac{1}{2} \sum_{i=1}^m \log(1 + \sigma^{-2} \lambda_i \eta_i)$ , with  $\lambda_i > 0$  and  $\sigma^2 > 0$ . Then the maximum of  $\Psi$  subject to  $\eta_i \geq 0$  and  $\sum \eta_i = m$  is obtained at*

$$\eta_i = \begin{cases} \frac{m}{k} - \sigma^2 \lambda_i^{-1} + \sigma^2 \frac{1}{k} \sum_{j \in A} \lambda_j^{-1} & i \in A \\ 0 & i \in A^c \end{cases} \tag{20}$$

where  $A := \{1 \leq i \leq m : \eta_i > 0\}$  and  $A^c = \{1, \dots, m\} \setminus A$ , and  $k = |A|$ , the cardinality of  $A$ .

The proof of Proposition 5.5 amounts to utilizing the Karush-Kuhn-Tucker conditions and is delegated to the Supplementary. The final ingredient we require for the proof of Theorem 5.7 characterizing D-optimal designs is:

**Lemma 5.6** (Unit norm decomposition). *Let  $M \in \mathbb{R}^{k \times k}$  symmetric positive definite with  $\text{tr } M = m$ ,  $m \geq k$ . We can find  $\mathbf{a}_j \in \mathbb{R}^k, j = 1, \dots, m$  with  $\|\mathbf{a}_j\| = 1$  and  $A = (\mathbf{a}_1, \dots, \mathbf{a}_m)$  such that  $AA^t = M$ .*

The proof of Lemma 5.6 is also delegated to the Supplementary. It is however important to note that this proof is constructive; it will allow us to construct D-optimal designs, once we fully characterize them in Theorem 5.7 below.

**Theorem 5.7.** *Let:*

- *The D-optimality design criterion [1]:*

$$\Psi(\mathcal{O}) = \frac{1}{2} \log \det(I + \sigma^{-2} \Gamma_{\text{pr}}^{1/2} \mathcal{F}^* \mathcal{O}^* \mathcal{O} \Gamma_{\text{pr}}^{1/2}),$$

- *D a D-optimal design operator*

$$\mathcal{D} = \underset{\|\mathbf{o}_j\|=1, j=1, \dots, m}{\arg \max} \Psi(\mathcal{O}),$$

- $\{\lambda_i\}_{i=1}^{\infty}$  *eigenvalues of  $\mathcal{F} \Gamma_{\text{pr}} \mathcal{F}^*$  in decreasing order of magnitude.*
- $\{\eta_i\}_{i=1}^{\infty}$  *eigenvalues of  $\mathcal{D}^* \mathcal{D}$ .*

*Then:*

1.  $\text{tr} \{\mathcal{D}^* \mathcal{D}\} = m$ .
2.  $\mathcal{D}^* \mathcal{D}$  and  $\mathcal{F} \Gamma_{\text{pr}} \mathcal{F}^*$  are simultaneously diagonalizable.
3.  $k := \text{rank } \mathcal{D}^* \mathcal{D} \leq m$  and

$$\Psi(\mathcal{D}) = \frac{1}{2} \sum_{i=1}^k \log(1 + \sigma^{-2} \lambda_i \eta_i).$$

4.

$$\eta_i = \begin{cases} \frac{m}{k} - \sigma^2 \lambda_i^{-1} + \sigma^2 \frac{1}{k} \sum_{j=1}^k \lambda_j^{-1} & 1 \leq i \leq k \\ 0 & i > k \end{cases}.$$

5. *The covariance of the pushforward  $\mathcal{F}_* \mu_{\text{post}}^{\mathbf{d}, \mathcal{D}}$  is  $((\mathcal{F} \Gamma_{\text{pr}} \mathcal{F}^*)^{-1} + \sigma^{-2} \mathcal{D}^* \mathcal{D})^{-1}$  and its eigenvalues are*

$$\theta_i = \begin{cases} \left( \frac{\sum_{j=1}^k \lambda_j^{-1} + \sigma^{-2} m}{k} \right)^{-1} & i \leq k \\ \lambda_i & i > k \end{cases}. \quad (21)$$

*Then:*

1.  $\text{tr} \{\mathcal{O}^* \mathcal{O}\} = m$ .
2.  $\mathcal{O}^* \mathcal{O}$  and  $\mathcal{F} \Gamma_{\text{pr}} \mathcal{F}^*$  are simultaneously diagonalizable.
3.  $k := \text{rank } \mathcal{O}^* \mathcal{O} \leq m$  and

$$\Psi(\mathcal{O}) = \frac{1}{2} \sum_{i=1}^k \log(1 + \sigma^{-2} \lambda_i \eta_i).$$

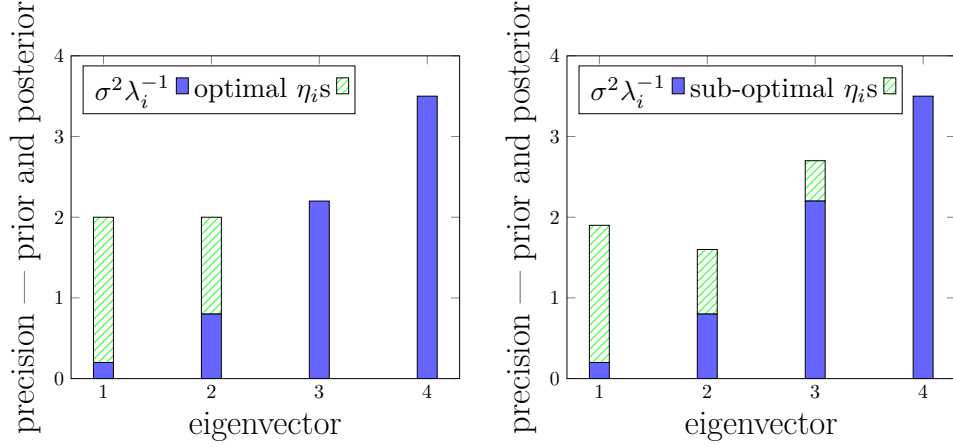


Figure 2: A comparison of the eigenvalues of the pushforward posterior precision  $(\mathcal{F}\Gamma_{\text{pr}}\mathcal{F}^*)^{-1} + \sigma^{-2}\mathcal{O}^*\mathcal{O}$  for a D-optimal design (left) and a sub-optimal design (right). Both designs are allowed  $m = 3$  measurements. We assume  $\sigma^2 = 1$  and thus, the blue area has accumulated height of  $\sigma^{-2}m = 3$  in both panels. The D-optimal design (left) increases precision where it is lowest. The sub-optimal design (right) does not.

4.

$$\eta_i = \begin{cases} \frac{m}{k} - \sigma^2\lambda_i^{-1} + \sigma^2\frac{1}{k}\sum_{j=1}^k\lambda_j^{-1} & 1 \leq i \leq k \\ 0 & i > k \end{cases}.$$

5. The covariance of the pushforward  $\mathcal{F}_*\mu_{\text{post}}$  is  $((\mathcal{F}\Gamma_{\text{pr}}\mathcal{F}^*)^{-1} + \sigma^{-2}\mathcal{O}^*\mathcal{O})^{-1}$  and its eigenvalues are

$$\theta_i = \begin{cases} \left(\frac{\sum_{j=1}^k\lambda_j^{-1} + \sigma^{-2}m}{k}\right)^{-1} & i \leq k \\ \lambda_i & i > k \end{cases}$$

*Proof.* Part (1) is immediate for any measurement operator  $\mathcal{O}$  that satisfies the unit norm constraint on measurements. Part (2) was proved in Proposition 5.3. Part (3) was proved in Proposition 5.4.

Part (4) is a consequence of Propositions 5.4 and 5.5, with the caveat that we did not show that finding  $\mathcal{D}$  so that  $\mathcal{D}^*\mathcal{D}$  has the desired eigenvalues is feasible. To this end, we utilize Lemma 5.6: let  $M = \text{diag}(\eta_1, \dots, \eta_k)$ , diagonal with respect to the first  $k$  eigenvectors of  $\mathcal{F}\Gamma_{\text{pr}}\mathcal{F}^*$ . We take  $\mathcal{D} := A$  from Lemma 5.6.

Recall from (7), that the posterior precision is  $\Gamma_{\text{post}}^{-1} = \Gamma_{\text{pr}}^{-1} + \sigma^{-2}\mathcal{F}^*\mathcal{D}^*\mathcal{D}\mathcal{F}$ . The first statement in part (5) now follows from Proposition 5.1, while the second statement follows from parts (1) and (4).  $\square$

Part (5) of Theorem 5.7 gives us deep understanding of D-optimal designs when  $\Gamma_{\text{model}} = 0$ : Imagine each eigenvector of the *precision*  $(\mathcal{F}\Gamma_{\text{pr}}\mathcal{F}^*)^{-1}$  corresponds to a graduated lab cylinder. cylinder  $i$  is filled, a-priori, with green liquid of  $\lambda_i^{-1}$  volume units. We are allowed  $m$  measurement, so we have blue liquid of volume  $\sigma^{-2}m$  units at our disposal. When we seek a D-optimal design, we distribute the blue liquid by repeatedly adding a drop to whatever cylinder currently has the lowest level of liquid in it, as long as its index  $i \leq m$ . The result of such a procedure is that the precision for the first  $k$  eigenvectors is the average of their total aggregated precision  $\sum_{j=1}^k \lambda_j^{-1} + \sigma^{-2}m$ , see eq. (21) and Fig. 2 for an illustration.

## 5.1 Answer to Question 3

Building on Theorem 5.7, we can now give a compelling explanation to the measurement clusterization we observed for the inverse problem of the heat equation, see Section 5.1 below. We also suggest a generic explanation for clusterization, see Section 5.1.

### Clusterization in the heat equation

Consider  $\mathcal{F}$  and  $\Gamma_{\text{pr}}$  from *the inverse problem of the heat equation*. As before, we denote the eigenvalues of  $\mathcal{F}\Gamma_{\text{pr}}\mathcal{F}^*$  by  $\lambda_j$ . We input these eigenvalues into our *generic* model, and find a D-optimal design  $\mathcal{D}$  for our generic model using Theorem 5.7. In our generic model, the measurements we take are best utilized in reducing uncertainty for the first  $k$  eigenvectors. So, a D-optimal design arising from our *generic model* completely avoids measuring eigenvectors  $k + 1$  and above.

Of course, in a real life problem — such as the inverse problem of the 1D heat equation — it is likely impossible to find measurements for which all eigenvectors  $k + 1$  and above are zero. However, if the eigenvalues of  $\mathcal{F}\Gamma_{\text{pr}}\mathcal{F}^*$  decay quickly (recall the square-exponential decay for eigenvalues of the 1D heat equation in eq.(3)), a D-optimal design will try to balance measuring a small number (i.e.  $k$ ) of the leading eigenvectors.

The abovementioned balance is explored in Fig. 5.1. We allow  $m = 4$  measurements in  $\Omega = [0, 1]$  and observe that D-optimal measurement locations are clustered at  $x_1 = 0.31$  and  $x_2 = 0.69$ . Upon close inspection of the scaled eigenvectors of  $\mathcal{F}\Gamma_{\text{pr}}\mathcal{F}^*$ , we first observe that eigenvectors 3 and above have negligible prior amplitude. Since we only have  $m = 4$  measurements at our disposal, we interpret these results, following Theorem 5.7, as implying we should only care about measuring the first and second eigenvectors. Then, we note the D-optimal  $x_1, x_2$  present a compromise between the amplitude of the first and second eigenvectors. For example, a measurement at  $x = 0.5$  would have ignored the second eigenvector altogether, since the second eigenvector is zero at  $x = 0.5$ .

Now we can understand measurement clusterization for the inverse problem of the 1D heat equation. A D-optimal design attempts to measure the first  $k$  eigenvectors of  $\mathcal{F}\Gamma_{\text{pr}}\mathcal{F}^*$ . But there may be (spatial) limitations on where these  $k$  eigenvectors have large amplitude. For the inverse problem of the heat equation there are two spatial locations that present a good compromise between the amplitudes of the first and second

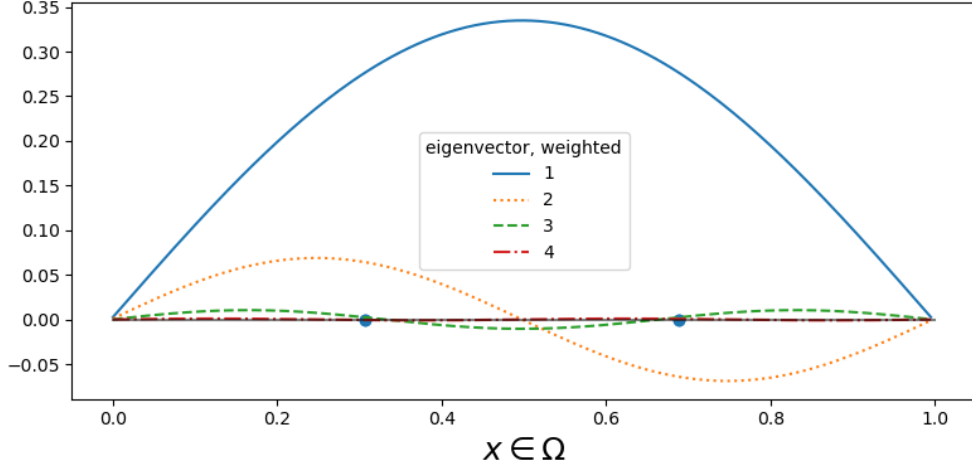


Figure 3: D-optimal measurement locations ( $m = 4$  measurements) and weighted eigenvectors for finding the initial condition of the 1D heat equation. Measurement locations and weighted eigenvectors are plotted over the computational domain  $\Omega = [0, 1]$  (x-axis). Measurement clusterization occurs approximately at 0.31 and 0.69. These two locations are a compromise between the amplitudes of the first and second eigenvectors, which are the eigenvectors that a D-optimal design aims to measure. Allocating  $m = 4$  measurements into two locations results in clusterization, according to the pigeonhole principle.

eigenvectors, namely  $x_1$  and  $x_2$  — see Fig. 5.1. We have  $m = 4$  measurements at our disposal but only two spatial locations that are a good compromise between the amplitudes of the first and second scaled eigenvectors. Thus, clusterization arises as a consequence of the pigeonhole principle.

### Clusterization in our generic model

We can gain further insight to clusterization in our generic model, from Carathéodory’s Theorem and the concentration on the first  $k$  eigenvectors of  $\mathcal{F}\Gamma_{\text{pr}}\mathcal{F}^*$ . We present a short discussion adapting arguments presented in [38, Chapter 3] and [33, Section 5.2.3].

Consider  $\mathcal{D}$  a D-optimal design under our generic model. As instructed by Theorem 5.7, we ignore all but the first  $k$  eigenvectors of  $\mathcal{F}\Gamma_{\text{pr}}\mathcal{F}$ . Thus, we replace  $\mathcal{H}_o$  with  $\mathcal{H}_o^{(k)}$  — the  $k$ -dimensional subspace spanned by the first  $k$  eigenvectors of  $\mathcal{F}^*\Gamma_{\text{pr}}\mathcal{F}$ . Let

$$\mathcal{M} := \text{conv}\{\mathbf{o}\mathbf{o}^* : \mathbf{o} \in \mathcal{H}_o^{(k)}, \|\mathbf{o}\| = 1\},$$

where  $\text{conv}$  denotes the convex hull of a set. The set  $\mathcal{M}$  contains only positive-definite operators on a  $k$ -dimensional vector space. Hence  $\mathcal{M}$  lives in a  $k(k+1)/2$ -dimensional

vector space. Since  $\mathcal{D}^*\mathcal{D} = \sum_{i=1}^m \mathbf{o}_i \mathbf{o}_i^*$  for  $\mathbf{o}_i \in \mathcal{H}_o^{(k)}$ , it is easy to verify that  $\frac{1}{m} \mathcal{D}^*\mathcal{D} \in \mathcal{M}$ . Recall Carathéodory's Theorem:

**Theorem** (Carathéodory). Let  $X \subseteq \mathbb{R}^n, X \neq \emptyset$  and denote  $\text{conv}(X)$  the convex hull of  $X$ . For every  $x \in \text{conv}(X)$ ,  $x$  is a convex combination of at most  $n + 1$  vectors in  $X$ .

Carathéodory's Theorem implies that there exist  $\mathbf{o}_i$  and  $\alpha_i$  such that

$$\mathcal{D}^*\mathcal{D} = \sum_{i=1}^I \alpha_i \mathbf{o}_i \mathbf{o}_i^*,$$

where  $\|\mathbf{o}_i\| = 1, \sum \alpha_i = m, \alpha_i \geq 0$  and  $I = \frac{k(k+1)}{2} + 1$ . We can thus write  $\mathcal{D}$  as:

$$\mathcal{D} = \begin{bmatrix} - & \sqrt{\alpha_1} \mathbf{o}_1^* & - \\ - & \sqrt{\alpha_2} \mathbf{o}_2^* & - \\ & \vdots & \\ - & \sqrt{\alpha_I} \mathbf{o}_I^* & - \end{bmatrix}.$$

Unfortunately,  $\mathcal{D}$  is not a valid design, since its rows do not have unit norm. Still, the above representation of  $\mathcal{D}$  is useful: If  $m > \frac{k(k+1)}{2} + 1$ , then  $\alpha_i > 1$  for some  $1 \leq i \leq I$ . Thus, we can view  $\mathcal{D}$  as a clustered design, since it places weight  $> 1$  on a single measurement vector.

## Convergence

In this section we fulfill our promise from Section 1.4 and prove that the posterior uncertainty ellipsoid in  $\mathcal{H}_o$  will contract to zero along every eigenvector of  $\mathcal{F}\Gamma_{\text{pr}}\mathcal{F}^*$ . In our proof we ignore potential problems with conducting inference on function spaces which are not unique to D-optimal designs (see e.g. [32] for more details).

First, denote  $\mathcal{D}_m$  a D-optimal design utilizing  $m$  measurements and denote  $k_m := \text{rank } \mathcal{D}_m^* \mathcal{D}_m$ . An immediate consequence of Theorem 5.7 is that allowing more measurements will eventually allow us to measure each eigenvalue, i.e.:

$$\lim_{m \rightarrow \infty} k_m = \infty \quad (22)$$

Now, recall that part (5) of Theorem 5.7 ensures that the eigenvalues of the posterior pushforward covariance equal

$$\theta_i^{(k)} = \left( \frac{\sum_{j=1}^k \lambda_j^{-1} + \sigma^{-2} m}{k} \right)^{-1}, \text{ for } i \leq k.$$

Using the inequality for the arithmetic and harmonic means, it is easy to verify that

$$\theta_i^{(k)} \leq \lambda_k.$$

Since  $\lim_{k \rightarrow \infty} \lambda_k = 0$ , we conclude that for all  $i$ ,  $\lim_{k \rightarrow \infty} \theta_i^{(k)} = 0$ . Combining the latter observation with eq. (22), we conclude that  $\lim_{m \rightarrow \infty} \theta_i^{(k_m)} = 0$  for all  $i$ . Therefore, posterior uncertainty decays to zero for all eigenvectors.

## 6 Numerical Experiments

### 6.1 Simulating Theorem 5.7

In the proof of Theorem 5.7 we utilize Lemma 5.6 to construct D-optimal designs. We implement this construction with the goal of testing numerically how prevalent are clustered designs. To this end, we would like to generate random prior eigenvalues  $\lambda_j$ , fix  $m$  and  $k$ , find what a D-optimal  $\mathcal{D}^* \mathcal{D}$  should be, and then utilize the construction of Theorem 5.7 and Lemma 5.6 to find  $\mathcal{D}$ .

To simplify things, we directly generate  $\mathcal{D}^* \mathcal{D}$ . We iterate over the number of measurements  $m \in \{4, \dots, 24\}$ , and for every  $m$  we then iterate over  $k := \text{rank } \mathcal{D}^* \mathcal{D} \in \{2, \dots, m - 1\}$ . For each pair  $m, k$  we repeat the following steps  $N = 5000$  times:

1. Generate random diagonal  $D \in \mathbb{R}^{k \times k}$  with entries  $\log(d_i) \sim \mathcal{N}(50, 15)$ .
2. Normalize  $D$  that  $\text{tr } D = m$ .
3. Conjugate  $D$  by a random orthogonal matrix to form a positive semi-definite  $M := UDU^t \in \mathbb{R}^{k \times k}$ . This  $M$  represents  $\mathcal{D}^* \mathcal{D}$ .
4. Apply the construction of Lemma 5.6 to calculate  $A$  such that  $AA^t = M$ , where  $A$  has unit norm columns.  $A^t$  is our optimal design  $\mathcal{D}$ .
5. Since  $A^t$  corresponds to  $\mathcal{D}$ , its columns correspond to measurement vectors. We call  $A$  "clustered" if  $A$  has two or more identical columns (up to some numerical precision threshold, i.e.  $10^{-5}$ ).

We then calculate the fraction of clustered designs of the simulations we ran, for each pair  $m, k$ . Clusterization occurred at high rates ( $> 99.9\%$ ) whenever  $m - k > 1$ ; see Fig. 4. Hence, in these simulations, clusterization is a generic property. However, when  $m - k = 1$ , clusterization does not occur. We do not why this is so.

Full results are located in the `simulations.csv` file within the accompanying [repository](#). Code implementing the experiments described above is located in module `zeros.py` of said repository. Runtime should be less than 30 minutes on any reasonably modern laptop (it took 12 minutes on the author's laptop).

### 6.2 Correlated errors

In order to verify the results of Section 4, we run simulations of the inverse problem of the 1D heat equation with nonvanishing model error  $\Gamma_{\text{model}} = \Gamma_{\text{pr}}^2$ . Indeed, including



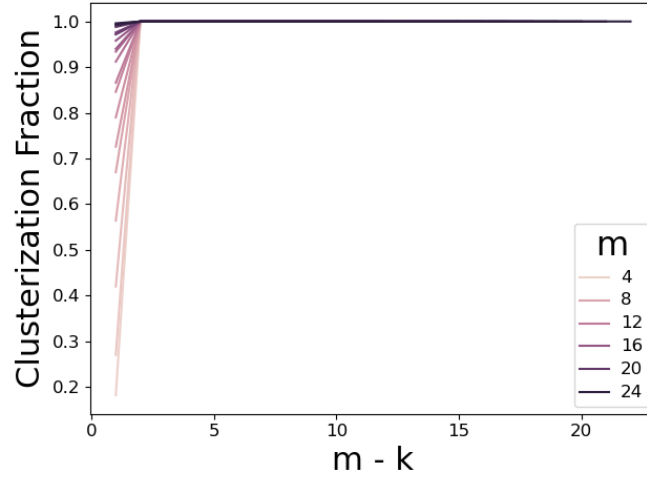


Figure 4: Fraction of clustered  $A$  for  $AA^t = M$  and  $M$  generated randomly (see text and repository for details on generating  $M$ ). It is evident that when  $m - k > 1$  clusterization is prevalent, whereas for lower  $m - k$  clusterization is not.

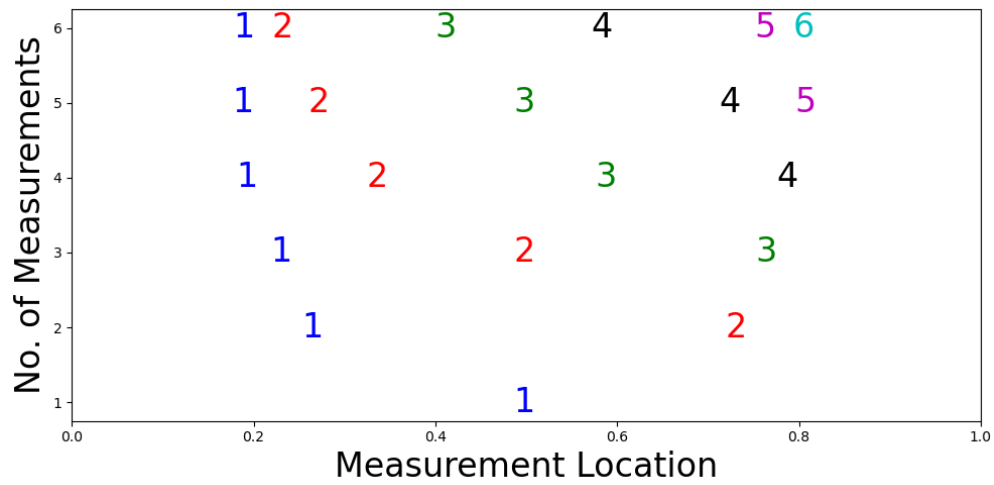


Figure 5: Model correlation mitigates clusterization. We add a model correlation term to the error terms in the 1D heat equation inverse problem. As expected, measurements are pushed away owing to the model error term.

model correlation pushes measurements apart, see Fig. 5. Code generating Fig. 5 is located in module `clusterization.py` in the accompanying [repository](#).

### Acknowledgments

This study is a result of research I started during my PhD studies under the instruction of Prof. Georg Stadler at the Courant Institute of Mathematical Sciences. I would like to thank him for his great mentorship, attention to details and kindness. I would also like to thank Christian Remling, who helped me find a proof for Lemma 5.6 in [Mathoverflow](#). Last, but certainly not least, I would like to thank the three referees, associate editor and editor in chief for providing detailed and insightful reviews that have made this manuscript a whole lot better.

### Funding

This research was supported in part by an appointment with the National Science Foundation (NSF) Mathematical Sciences Graduate Internship (MSGI) Program sponsored by the NSF Division of Mathematical Sciences. This program is administered by the Oak Ridge Institute for Science and Education (ORISE) through an interagency agreement between the U.S. Department of Energy (DOE) and NSF. ORISE is managed for DOE by ORAU. All opinions expressed in this paper are the author's and do not necessarily reflect the policies and views of NSF, ORAU/ORISE, or DOE.

## References

- [1] Alen Alexanderian, Philip J. Gloor, and Omar Ghattas. On Bayesian A- and D-optimal experimental designs in infinite dimensions. *Bayesian Analysis*, 11(3):671–695, 2016. [3](#), [11](#), [12](#), [19](#)
- [2] Alen Alexanderian, Noemi Petra, Georg Stadler, and Omar Ghattas. A-optimal design of experiments for infinite-dimensional bayesian linear inverse problems with regularized  $\ell_0$ -Sparsification. *SIAM Journal on Scientific Computing*, 36(5):A2122–A2148, 2014. [6](#), [7](#)
- [3] Alen Alexanderian, Noemi Petra, Georg Stadler, and Omar Ghattas. A fast and scalable method for A-optimal design of experiments for infinite-dimensional bayesian nonlinear inverse problems. *SIAM Journal on Scientific Computing*, 38(1):A243–A272, 2016. [6](#), [7](#)
- [4] Alen Alexanderian, Noemi Petra, Georg Stadler, and Isaac Sunseri. Optimal design of large-scale Bayesian linear inverse problems under reducible model uncertainty: Good to know what you don't know. *SIAM/ASA Journal on Uncertainty Quantification*, 9(1):163–184, 2021. [6](#)
- [5] Alen Alexanderian and Arvind K Saibaba. Efficient D-optimal design of experiments for infinite-dimensional Bayesian linear inverse problems. *SIAM Journal on Scientific Computing*, 40(5):A2956–A2985, 2018. [6](#), [11](#), [12](#)
- [6] Ahmed Attia and Emil Constantinescu. Optimal Experimental Design for Inverse

- Problems in the Presence of Observation Correlations. *SIAM Journal on Scientific Computing*, 44(4):A2808–A2842, August 2022. 6
- [7] Ahmed Attia, Sven Leyffer, and Todd S Munson. Stochastic learning approach for binary optimization: Application to Bayesian optimal design of experiments. *SIAM Journal on Scientific Computing*, 44(2):B395–B427, 2022. 7
- [8] Michael Brin and Garrett Stuck. *Introduction to Dynamical Systems*. Cambridge university press, 2002. 10
- [9] B. W. Brunton, S. L. Brunton, J. L. Proctor, and J. N. Kutz. Sparse Sensor Placement Optimization for Classification. *SIAM Journal on Applied Mathematics*, 76(5):2099–2122, January 2016. 6
- [10] Kathryn Chaloner and Isabella Verdinelli. Bayesian experimental design: A review. *Statistical Science*, 10(3):273–304, 1995. 1, 3
- [11] Barry A. Cipra. An Introduction to the Ising Model. *The American Mathematical Monthly*, 94(10):937–959, 1987. 10
- [12] Thomas M Cover and Joy A Thomas. *Elements of Information Theory*. John Wiley & Sons, 1999. 3
- [13] Philip A. Fay, Jonathan D. Carlisle, Alan K. Knapp, John M. Blair, and Scott L. Collins. Altering Rainfall Timing and Quantity in a Mesic Grassland Ecosystem: Design and Performance of Rainfall Manipulation Shelters. *Ecosystems*, 3(3):308–319, May 2000. 5
- [14] Valerii V. Fedorov. Design of spatial experiments: Model fitting and prediction. Technical Report TM-13152, Oak Ridge National Lab, Oak Ridge, Tennessee, March 1996. 4, 6, 9
- [15] Valerii V. Fedorov and Peter Hackl. *Model-Oriented Design of Experiments*, volume 125 of *Lecture Notes in Statistics*. Springer, New York, NY, 1997. 4, 6
- [16] Ronald A Fisher. The design of experiments. 1949. 5
- [17] E Haber, L Horesh, and L Tenorio. Numerical methods for experimental design of large-scale linear ill-posed inverse problems. *Inverse Problems*, 24(5):055012, September 2008. 2, 7
- [18] Lior Horesh, Eldad Haber, and Luis Tenorio. Optimal experimental design for the large-scale nonlinear ill-posed problem of impedance imaging. In *Large-Scale Inverse Problems and Quantification of Uncertainty*, pages 273–290. John Wiley & Sons, Ltd, 2010. 2
- [19] Bamdad Hosseini. Well-Posed Bayesian Inverse Problems with Infinitely Divisible and Heavy-Tailed Prior Measures. *SIAM/ASA Journal on Uncertainty Quantification*, 5(1):1024–1060, January 2017. 9
- [20] Bamdad Hosseini. Two Metropolis–Hastings Algorithms for Posterior Measures with Non-Gaussian Priors in Infinite Dimensions. *SIAM/ASA Journal on Uncertainty Quantification*, 7(4):1185–1223, January 2019. 9

- [21] Jari P. Kaipio and Erkki Somersalo. *Statistical and Computational Inverse Problems*, volume 160 of *Applied Mathematical Sciences*. Springer, New York, NY, 2005. [2](#), [11](#)
- [22] Mehran Kardar. *Statistical Physics of Particles*. Cambridge University Press, Cambridge, 2007. [10](#)
- [23] B. T. Knapik, A. W. van der Vaart, and J. H. van Zanten. Bayesian Inverse Problems with Gaussian Priors. *The Annals of Statistics*, 39(5):2626–2657, 2011. [9](#), [10](#)
- [24] Karina Koval, Alen Alexanderian, and Georg Stadler. Optimal experimental design under irreducible uncertainty for linear inverse problems governed by PDEs. *Inverse Problems*, 36(7):075007, June 2020. [6](#), [9](#)
- [25] Finn Lindgren, Håvard Rue, and Johan Lindström. An explicit link between Gaussian fields and Gaussian Markov random fields: The stochastic partial differential equation approach. *Journal of the Royal Statistical Society: Series B (Statistical Methodology)*, 73(4):423–498, 2011. [4](#)
- [26] John David Logan. *A First Course in Differential Equations*. Springer, 2006. [10](#)
- [27] Ben Marson, Raya Horesh, Lior Horesh, and DS Holder. A new protocol for the rapid generation of accurate anatomically realistic finite element meshes of the head from T1 MRI scans. In *Proc. of IX Int. Conf. on Electrical Impedance Tomography (Hanover, NH, USA)*, pages 44–7, 2008. [2](#)
- [28] Max Morris. *Design of Experiments: An Introduction Based on Linear Models*. Chapman and Hall/CRC, New York, July 2011. [5](#)
- [29] Ira Neitzel, Konstantin Pieper, Boris Vexler, and Daniel Walter. A sparse control approach to optimal sensor placement in PDE-constrained parameter estimation problems. *Numerische Mathematik*, 143(4):943–984, 2019. [4](#), [6](#), [9](#)
- [30] Richard Nickl. *Bayesian Non-Linear Statistical Inverse Problems*. EMS press, 2023. [9](#)
- [31] Joakim Nyberg, Richard Höglund, Martin Bergstrand, Mats O. Karlsson, and Andrew C. Hooker. Serial correlation in optimal design for nonlinear mixed effects models. *Journal of Pharmacokinetics and Pharmacodynamics*, 39(3):239–249, June 2012. [4](#), [6](#)
- [32] Houman Owhadi, Clint Scovel, and Tim Sullivan. On the Brittleness of Bayesian Inference. *SIAM Review*, 57(4):566–582, January 2015. [23](#)
- [33] Luc Pronzato and Andrej Pázman. *Design of Experiments in Nonlinear Models: Asymptotic Normality, Optimality Criteria and Small-Sample Properties*, volume 212 of *Lecture Notes in Statistics*. Springer, New York, NY, 2013. [22](#)
- [34] Nitzan Rabinowitz and David M. Steinberg. Optimal configuration of a seismographic network: A statistical approach. *Bulletin of the Seismological Society of America*, 80(1):187–196, February 1990. [2](#)

- [35] Michael Renardy and Robert C Rogers. *An Introduction to Partial Differential Equations*, volume 13. Springer Science & Business Media, 2006. [4](#)
- [36] Kenneth J Ryan. Estimating expected information gains for experimental designs with application to the random fatigue-limit model. *Journal of Computational and Graphical Statistics*, 12(3):585–603, 2003. [9](#)
- [37] William D Schafer. Replication: A design principle for field research. *Practical Assessment, Research, and Evaluation*, 7(1):15, 2001. [5](#)
- [38] Samuel David Silvey. *Optimal Design*. Springer Netherlands, Dordrecht, 1980. [22](#)
- [39] David M. Steinberg, Nitzan Rabinowitz, Yair Shimshoni, and Daphna Mizrahi. Configuring a seismographic network for optimal monitoring of fault lines and multiple sources. *Bulletin of the Seismological Society of America*, 85(6):1847–1857, December 1995. [2](#)
- [40] Andrew M Stuart. Inverse problems: A bayesian perspective. *Acta numerica*, 19:451–559, 2010. [4](#), [10](#), [11](#)
- [41] Albert Tarantola. *Inverse Problem Theory and Methods for Model Parameter Estimation*. Other Titles in Applied Mathematics. Society for Industrial and Applied Mathematics, 2005. [2](#), [11](#)
- [42] Aretha L. Teckentrup. Convergence of Gaussian Process Regression with Estimated Hyper-Parameters and Applications in Bayesian Inverse Problems. *SIAM/ASA Journal on Uncertainty Quantification*, 8(4):1310–1337, January 2020. [9](#)
- [43] Jacqueline K Telford. A brief introduction to design of experiments. *Johns Hopkins apl technical digest*, 27(3):224–232, 2007. [5](#)
- [44] Dariusz Ucinski. *Optimal Measurement Methods for Distributed Parameter System Identification*. CRC Press, Boca Raton, 2005. [4](#), [5](#), [6](#), [15](#)
- [45] Curtis R. Vogel. *Computational Methods for Inverse Problems*. Society for Industrial and Applied Mathematics, 2002. [11](#)